

## On the pattern formation mechanism of (2+1)D max-plus models

This article has been downloaded from IOPscience. Please scroll down to see the full text article.

2001 J. Phys. A: Math. Gen. 34 10715

(<http://iopscience.iop.org/0305-4470/34/48/333>)

View [the table of contents for this issue](#), or go to the [journal homepage](#) for more

Download details:

IP Address: 171.66.16.101

The article was downloaded on 02/06/2010 at 09:46

Please note that [terms and conditions apply](#).

# On the pattern formation mechanism of (2 + 1)D max-plus models

Daisuke Takahashi, Atsuhiko Shida and Motohiro Usami

Department of Mathematical Sciences, Waseda University, 3-4-1, Ohkubo, Shinjuku-ku, Tokyo 169-8555, Japan

E-mail: daisuke@mse.waseda.ac.jp

Received 14 April 2001, in final form 16 June 2001

Published 23 November 2001

Online at [stacks.iop.org/JPhysA/34/10715](http://stacks.iop.org/JPhysA/34/10715)

## Abstract

We propose a max-plus equation which reproduces evolutionary patterns often observed in reaction–diffusion systems of excitable media. The equation gives a travelling wave, a target pattern and a spiral pattern from appropriate initial data. Moreover, using the advantages of max-plus equations, we obtain the solutions exactly by a reduction from the high-dimensional equation to a lower one. In the reduction, we use coordinate curves according to a pattern shape. It is interesting that all patterns satisfy the same reduced equation. We also propose two other models similar to the previous one and discuss the behaviour of solutions.

PACS numbers: 45.70.Qj, 05.45.-a, 47.54.+r

## 1. Introduction

Max-plus algebra is constructed from max operation as ‘addition’ and addition as ‘multiplication’ [1]. The following shows the correspondence between the usual real number operations and max-plus operations:

$$\begin{aligned}
 a + b & \leftrightarrow \max(A, B), \\
 ab & \leftrightarrow A + B, \\
 a/b & \leftrightarrow A - B, \\
 a + (b + c) = (a + b) + c & \leftrightarrow \max(A, \max(B, C)) = \max(\max(A, B), C) \\
 & \qquad \qquad \qquad = \max(A, B, C), \\
 a(bc) = (ab)c & \leftrightarrow A + (B + C) = (A + B) + C, \\
 a(b + c) = ab + ac & \leftrightarrow A + \max(B, C) = \max(A + B, A + C).
 \end{aligned}$$

Since ‘subtraction’ ( $a - b$ ) is not defined in max-plus algebra without a special condition, we cannot automatically transform an equation and its solutions including four arithmetic

operations into those including max-plus operations. However, various ‘integrable’ max-plus equations were found by taking an ultradiscrete limit of integrable difference equations using the following formulae [2–5]:

$$\begin{aligned} \lim_{\varepsilon \rightarrow +0} \varepsilon \log(e^{A/\varepsilon} + e^{B/\varepsilon} + \dots) &= \max(A, B, \dots) \\ (\lim_{\varepsilon \rightarrow +0} )\varepsilon \log(e^{A/\varepsilon} e^{B/\varepsilon} \dots) &= A + B + \dots \end{aligned} \quad (1)$$

Difference special solutions like  $N$ -soliton solutions can also be transformed into max-plus ones. Though max-plus solutions can be derived from the corresponding difference ones, we can confirm that they satisfy the equation by a direct substitution using max-plus operations.

Another feature of the max-plus equation is the discreteness of its dependent variable. Let us consider the ultradiscrete Burgers equation [6]

$$U_j^{t+1} = U_{j-1}^t + \max(1, U_j^t + U_{j+1}^t) - \max(1, U_{j-1}^t + U_j^t)$$

as an example. (It can be ‘linearized’ using an ultradiscrete Cole–Hopf transformation  $U_j^t = F_{j+1}^t - F_j^t + 1/2$  and we obtain  $F_j^{t+1} = \max(F_{j-1}^t, F_{j+1}^t)$ .) We can consider that the dependent variable  $U$  is continuous, but if the initial values are all integers,  $U$  are always integer. In this sense, max-plus algebra can propose equations with all discrete variables. Moreover, we can easily show any  $U$  is always 0 or 1 if the initial  $U$  values are also. It means the above equation can become a cellular automaton (CA) [7].

Considering the above features of max-plus equations, we arrive at the following question: ‘How many mechanisms in continuous mathematics survive in max-plus algebra?’ Note that integrability is not necessary for max-plus operations. In this paper, we make max-plus models of a pattern formation mechanism, which give evolutionary patterns often observed in reaction–diffusion systems of excitable media.

Reaction–diffusion systems show us a rich structure of pattern dynamics [8]. For example, in the Belousov–Zhabotinsky (BZ) chemical reaction, two-dimensional ring-shaped reaction waves are repeatedly produced from a core area and they propagate outward as concentric circles [9]. This pattern is called a ‘target’ pattern. Moreover, a single- or a double-‘spiral’ pattern often appears. It turns around a core and its outer part propagates outward. The target and the spiral patterns are commonly observed in various reaction–diffusion systems. The systems are often modelled using two kinds of material, activator and inhibitor, in the form of a couple of differential equations. Numerical simulations of the model equations can reproduce the pattern dynamics well.

Moreover, various CA models have been made to simulate the dynamics [10–17]. They are discrete analogues to pattern formation systems and their results match the phenomena well. Due to the discreteness of CA models, we can obtain exact solutions even by numerical simulations. The local behaviour of solutions can be easily checked by analysing an evolution rule of the models. These are advantages of CA models. However, it is often difficult to discuss global or asymptotic properties of solutions in the CA models. On the other hand, we have accumulated many techniques to evaluate such properties for differential models. Our main purpose in this paper is to propose max-plus models including the advantages of both the CA and differential models. In the max-plus models, we can give exact solutions like those to CA models and can also show global behaviour of the solutions using similar techniques to those of differential models.

In section 2, we propose a  $(2+1)$ D max-plus model and show that it has various solutions including target and spiral patterns. In section 3, we show that basic solutions to the model can be derived from a lower-dimensional equation obtained by a reduction using some coordinate curves. The travelling wave, target pattern and spiral pattern are all derived from solutions to the same 1D equation reduced by corresponding curves. In section 4, we show two other

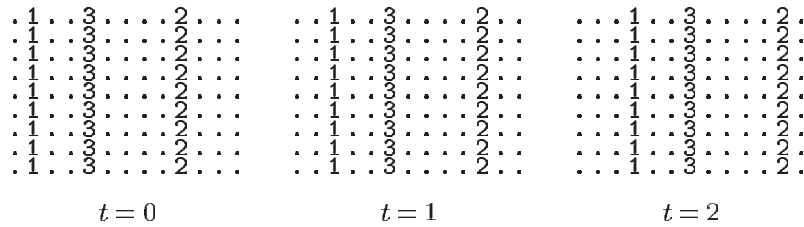


Figure 1. Travelling waves. A dot denotes 0.

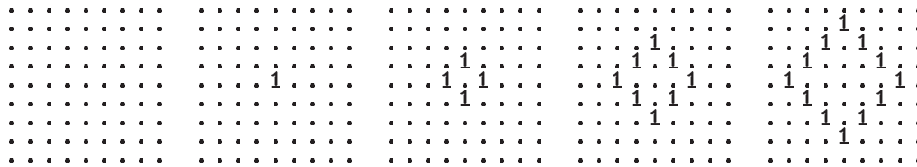


Figure 2. Single-ring pattern.

models obtained by a small modification of the original one. Though the shape and behaviour of the above basic solutions are slightly changed, they also exist stably in the models. In section 5, we give concluding discussions.

### 2. (2 + 1)D max-plus model

In this paper, we consider the following (2 + 1)D max-plus equation:

$$U_{ij}^{t+1} = \max(U_{i-1j}^t, U_{i+1j}^t, U_{ij-1}^t, U_{ij+1}^t, U_{ij}^t) - U_{ij}^t - U_{ij}^{t-1} \tag{2}$$

where  $i$  and  $j$  are both spatial lattices and  $t$  is the discrete time. We assume spatial lattices are infinite ( $-\infty < i < \infty$  and  $-\infty < j < \infty$ ) and  $U_{ij}^t \rightarrow 0$  for  $|i|, |j| \rightarrow \infty$ . Then we can follow a time evolution of  $U$  if we set initial data at two successive timesteps. Moreover, since (2) is symmetric on  $t$ , (2) is reversible in time.

Below we assume without loss of generality that  $t = 0$  is an initial time for the initial value problem of (2). If  $U_{ij}^0$  and  $U_{ij}^1$  are all integer valued, then  $U_{ij}^t$  is always an integer. In this sense, we can consider the dependent variable  $U$  as well as independent variables  $i, j$  and  $t$  are all discrete. Moreover, if  $U$  is a solution to (2),  $cU$  is also where  $c$  is a constant. Using this property and considering piecewise linearity of (2), we easily see that an initial value problem using integer values is equivalent to that using rational ones. Therefore, we can discuss the behaviour of a wide range of solutions by investigating only integer solutions.

Figure 1 shows an example of a basic solution to (2). Values 1, 2 and 3 make vertical lines respectively, with enough zeros between them, and initial data satisfy  $U_{ij}^1 = U_{i-1j}^0$ . Then, a solution obtained always satisfies  $U_{ij}^{t+1} = U_{i-1j}^t$ . Thus the non-zero lines become travelling waves with speed (1, 0), not interacting with each other. If we set initial data at  $t = 1$  by  $U_{ij}^1 = U_{i+1j}^0$ , then travelling waves with speed (-1, 0) are obtained. Generally, there are waves travelling in directions  $(\pm 1, 0)$  or  $(0, \pm 1)$  from appropriate initial data.

Figure 2 shows a ‘single-ring’ pattern.  $U_{ij}^0$  and  $U_{ij}^1$  are all 0 except that  $U_{ij}^1$  at a certain lattice point is 1. From that point, a diamond-shaped wave with value 1 spreads outward.

Figure 3 shows a process to form a stable ‘target’ pattern. At the centre point, the value changes periodically as 1, 1, -1 and diamond-shaped waves appear and spread outward repeatedly with period 3.

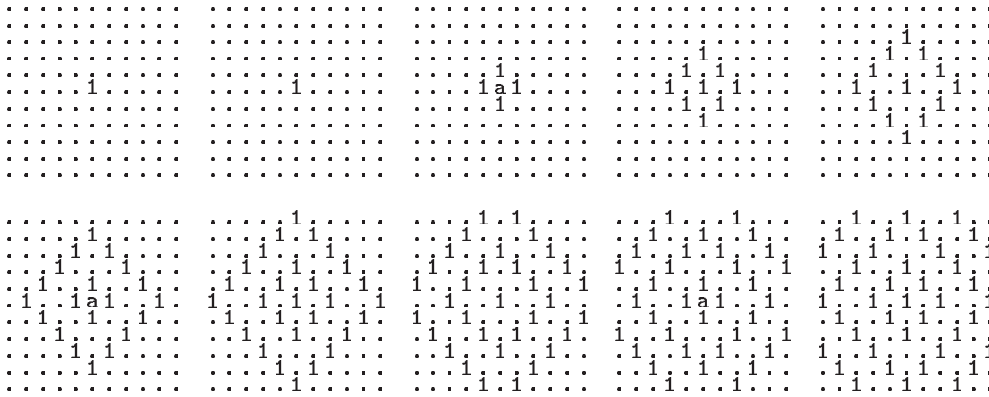


Figure 3. Target pattern. 'a' denotes  $-1$ .

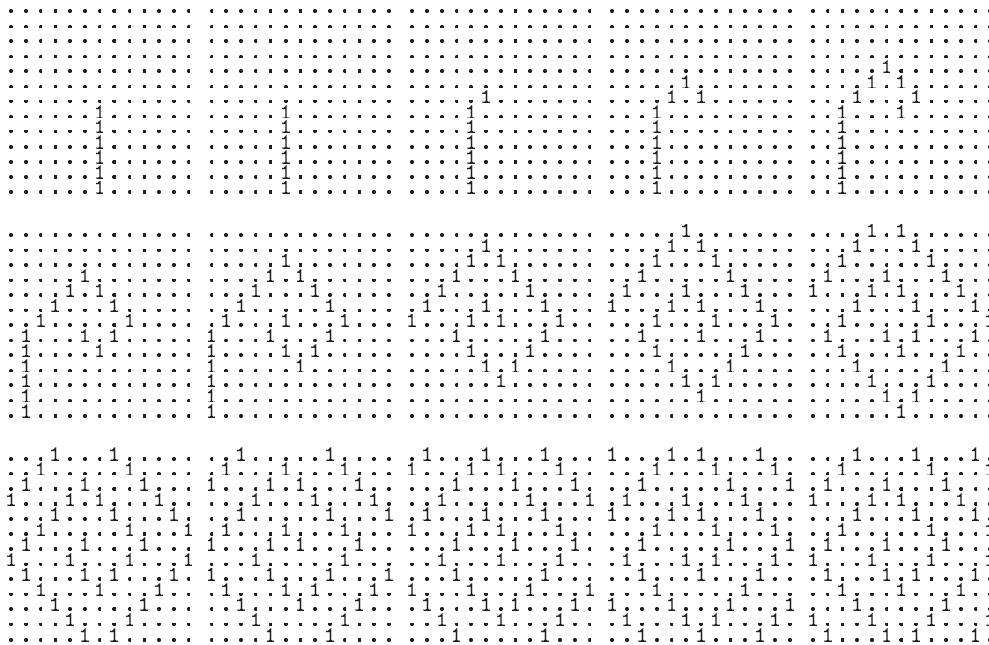


Figure 4. Spiral pattern.

Figure 4 shows a process to form a stable 'spiral' pattern. From an infinite line of value 1, we obtain a simple travelling wave like those in figure 1. If we use a half-line instead, a spiral appears from its end point. After an infinite time, the spiral spreads through the whole space region and it rotates by  $90^\circ$  per unit time.

We can consider the above target and spiral patterns are discrete analogues to those commonly observed in various reaction–diffusion systems. In the systems, the activator and inhibitor play important roles in making patterns. For example, the BZ reaction system is often modelled in the form

$$\begin{aligned} u_t &= D_u \Delta u + f(u, v) \\ v_t &= D_v \Delta v + g(u, v) \end{aligned} \quad (3)$$

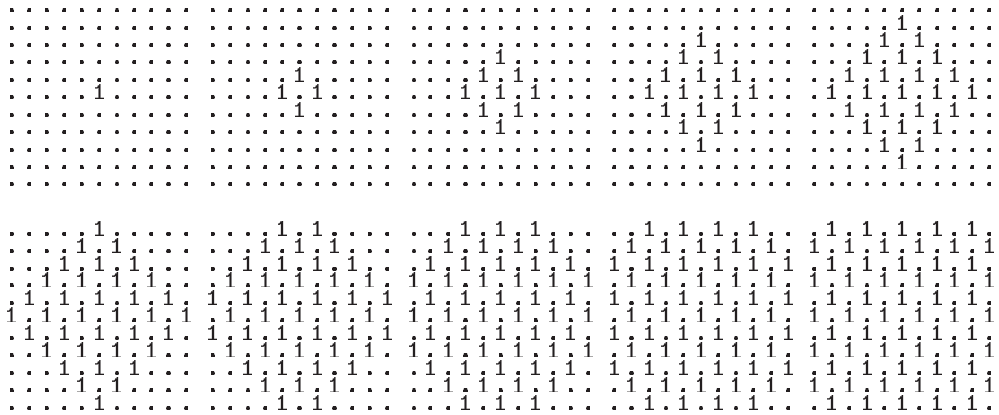


Figure 5. Time evolution of a solution to (5).

where  $D_u$  and  $D_v$  are diffusion coefficients and  $f$  and  $g$  are reaction terms [8]. State variables  $u(x, y, t)$  and  $v(x, y, t)$  are the ‘activator’ and ‘inhibitor’, respectively. Equation (3) is a system of first-order differential equations in time.  $D_u \Delta u$  and  $D_v \Delta v$  have a two-dimensional diffusion effect and  $f$  and  $g$  have a reaction effect between  $u$  and  $v$ . On the other hand, (2) is a single difference equation of second order in time. We can rewrite (2) as the following couple of equations using an auxiliary variable  $V_{ij}^t = U_{ij}^{t-1}$ ;

$$\begin{aligned} U_{ij}^{t+1} &= \max(U_{i-1j}^t, U_{i+1j}^t, U_{ij-1}^t, U_{ij+1}^t, U_{ij}^t) - U_{ij}^t - V_{ij}^t \\ V_{ij}^{t+1} &= U_{ij}^t. \end{aligned} \tag{4}$$

Both equations are of first order in time. Since the max term in the first equation includes von Neumann neighbourhoods of  $U_{ij}^t$ , information on a lattice point propagates to surrounding ones. Let us consider the following equation:

$$U_{ij}^{t+1} = \max(U_{i-1j}^t, U_{i+1j}^t, U_{ij-1}^t, U_{ij+1}^t, U_{ij}^t) - U_{ij}^t \tag{5}$$

which is made from the first equation of (4) by removing the last term in its right-hand side. If we set  $U_{ij}^0 = 0$  other than  $U_{00}^0 = 1$ , then we obtain a time evolution as shown in figure 5. We easily see from (5) that  $U_{ij}^{t+1} \geq 0$  generally, and a localized positive value of  $U$  spreads outward. In this rough meaning,  $U$  can be regarded as an activator.

The existence of  $V$  in the first equation of (4) means that  $U$  at the next time decreases if a current  $V$  is positive. Moreover, though current  $V$  is 0,  $V$  grows if current  $U$  is positive, according to the second equation. It means  $V$  plays the role of an inhibitor.

From the above discussion, we can consider that (4) is a rough sketch of the reaction–diffusion system. However, the above arguments are only the bare minimum of the reaction–diffusion system. They do not fully account for the occurrence of target and spiral patterns. In the next section, we further discuss the reason why both patterns appear in (2).

### 3. Stable pattern and coordinate curves

When we derive a special solution to a high-dimensional differential equation, we often assume a symmetry of solution and obtain a lower-dimensional differential equation. For example, if we have a (2 + 1)D PDE on  $u(x, y, t)$  and assume an axisymmetric solution, we usually assume  $u = v(r, t)$  with polar coordinate  $(r, \theta)$ , and reduce the (2 + 1)D PDE to (1 + 1)D. Moreover, if we were to get a travelling wave solution for  $v(r, t)$ , we assume  $v(r, t) = w(z)$

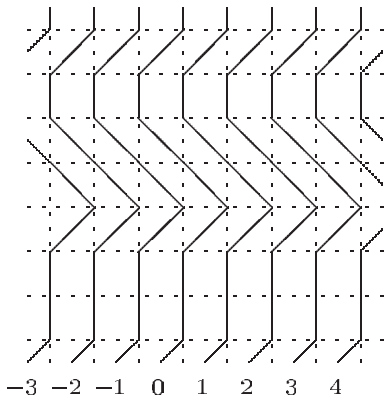


**Figure 6.** Example of a family of polygonal curves. Integers denote labels of the curves.

where  $z = r - ct$  and obtain an ODE on  $z$  from the  $(1 + 1)$ D PDE. We can show below that a similar procedure can be applied to (2) and all patterns in figures 1–4 satisfy the same ordinary difference equation.

Let us consider a family of lines defined by  $i = \text{const}$  and label each line by its  $i$ -coordinate. Moreover, if we assume that values of  $U_{ij}^0$  on the  $n$ th line are the same and that those of  $U_{ij}^1$  are also, values of  $U_{ij}^t$  on the  $n$ th line are always the same according to (2). Then, if  $F_n^t$  denotes the same value of  $U_{ij}^t$  on the  $n$ th line at time  $t$ ,  $F_n^t$  satisfies the following equation:

$$F_n^{t+1} = \max(F_{n-1}^t, F_n^t, F_{n+1}^t) - F_n^t - F_n^{t-1} \tag{6}$$

because  $\max(U_{i-1j}^t, U_{i+1j}^t, U_{ij-1}^t, U_{ij+1}^t, U_{ij}^t)$  reduces to  $\max(F_{n-1}^t, F_n^t, F_{n+1}^t)$ .

Moreover, if we consider a travelling wave solution  $F_n^t = G_{n \pm t}$  with speed  $\mp 1$ ,  $G_n$  satisfies

$$G_{n-1} + G_n + G_{n+1} = \max(G_{n-1}, G_n, G_{n+1}) \tag{7}$$

by a reduction of (6). This equation does not determine a solution uniquely from initial data. To obtain a general solution to (7), let us consider the following equation for  $A, B$  and  $C$ :

$$A + B + C = \max(A, B, C) \tag{8}$$

where  $A \leq B \leq C$ . Since the value of the right-hand side is equal to  $C$ ,  $A + B = 0$  is derived. Therefore, we obtain  $(A, B, C) = (-\alpha, \alpha, \beta)$  where  $0 \leq \alpha \leq \beta$ . Thus, if  $G_{n-1}, G_n$  and  $G_{n+1}$  satisfy a local condition

$$\{G_{n-1}, G_n, G_{n+1}\} = \{-\alpha, \alpha, \beta\} \tag{9}$$

for any  $n$ ,  $G$  becomes a solution to (7). Since a boundary condition on  $U$  is  $\lim_{|i|, |j| \rightarrow \infty} U_{ij}^t = 0$ , that for  $G$  is  $\lim_{|n| \rightarrow \infty} G_n = 0$ . Therefore, a general solution to (7) considering the boundary condition has a pattern of values as follows:

$$\dots 000p_10 * 0p_20 * 0p_30 * \dots * 0p_m000 \dots$$

where  $p_1, p_2, \dots, p_m$  are all positive numbers and  $*$  means nothing or some zeros. As for the solution in figure 1,  $G = \dots 000100300002000 \dots$ .

Other travelling wave solutions to (2) can be obtained by other symmetries of a solution. Consider a family of polygonal curves of infinite length reaching  $j \rightarrow \pm\infty$  as shown in figure 6. All curves have the same shape and all vertices are on lattice points. Moreover, all segments on a curve are any of  $(i, j) - (i - 1, j + 1)$ ,  $(i, j) - (i, j + 1)$  or  $(i, j) - (i - 1, j + 1)$ .

Let us label the curves sequentially with integers as shown in the figure. If we assume that all values of  $U_{ij}^t$  on each curve are the same,  $F_n^t$  denoting the value of  $U$  on a curve  $n$  at time  $t$  satisfies (6) because  $\max(U_{i-1j}^t, U_{i+1j}^t, U_{ij-1}^t, U_{ij+1}^t, U_{ij}^t)$  again reduces

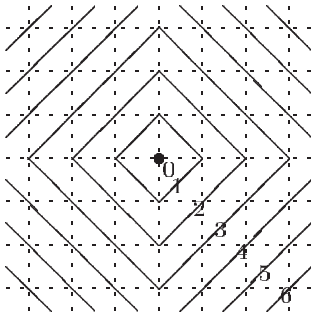


Figure 7. Family of diamond-shaped curves.

	$n=0$	1	2	3	4
$t=0$	0	0	0	0	0
1	1	0	0	0	0
2	0	1	0	0	0
3	0	0	1	0	0
4	0	0	0	1	0

(a)

	$n=0$	1	2	3	4	5	6	7	8	9
$t=0$	1	0	0	0	0	0	0	0	0	0
1	1	0	0	0	0	0	0	0	0	0
2	-1	1	0	0	0	0	0	0	0	0
3	1	0	1	0	0	0	0	0	0	0
4	1	0	0	1	0	0	0	0	0	0
5	-1	1	0	0	1	0	0	0	0	0
6	1	0	1	0	0	1	0	0	0	0
7	1	0	0	1	0	0	1	0	0	0
8	-1	1	0	0	1	0	0	1	0	0

(b)

Figure 8. Evolution of  $F_n^t$ . (a) Single ring, (b) target pattern.

to  $\max(F_{n-1}^t, F_n^t, F_{n+1}^t)$ . Moreover, we can obtain a travelling wave solution  $F_n^t = G_{n\pm t}$  satisfying (7). Note that there are travelling wave solutions obtained by rotating the solutions shown above by  $90^\circ$ .

Surprisingly, single-ring (figure 2), target (figure 3) and spiral (figure 4) patterns obey the same scenario as above. First, let us consider a family of diamond-shaped curves as shown in figure 7 and give a sequential integer as a label to each diamond. The centre point is a special diamond with zero area.

Consider an arbitrary lattice point  $(i, j)$  on the  $n$ th ( $n > 0$ ) diamond. Then, lattice points  $(i \pm 1, j)$  and  $(i, j \pm 1)$  are all on the  $(n - 1)$ th or  $(n + 1)$ th diamond and both diamonds include at least one point among the points. Therefore, if we assume that values of  $U_{ij}^t$  on each diamond are the same,  $F_n^t$  denoting the value of  $U$  on the  $n$ th diamond at time  $t$  satisfies (6) for  $n > 0$ . As for the centre point, a boundary condition

$$F_0^{t+1} = \max(F_0^t, F_1^t) - F_0^t - F_0^{t-1} \tag{10}$$

is applied. Under this condition, the evolution pattern of  $F_n^t$  for a single ring and a target pattern are shown in figures 8(a) and (b), respectively. Only one wave is produced from the point  $n = 0$  in the case of (a) and an infinite number of waves are periodically produced in the case of (b). Since a relation  $F_n^{t+1} = F_{n-1}^t$  is satisfied for  $n \geq 1$  in (a) and for  $n \geq 2$  in (b), we can consider that travelling waves are produced from a boundary condition on the point  $n = 0$ .

Secondly, let us consider a family of four spiral curves as shown in figure 9. They have the same shape and cover all lattice points in the plane. Nearest-neighbouring points of any point on a curve  $n$  are on a curve  $n - 1$  or  $n + 1$  modulo 4. Therefore, if we assume all  $U$  on each curve are the same, (2) reduces to (6) through  $F_n^t$  denoting a value of  $U$  on a curve  $n$  at time  $t$ . The variable  $n$  of  $F_n^t$  is periodic with period 4 or finite with modulus 4. Again we can consider a travelling wave solution  $F_n^t = G_{n\pm t}$  and it satisfies (7). Since there is a



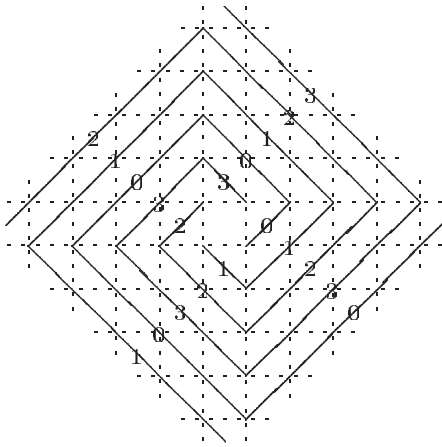


**Figure 9.** Four spiral curves.

restriction (9) for  $G_n$ , we obtain  $\{G_0, G_1, G_2, G_3\} = \{0, 0, 0, \alpha\}$  where  $\alpha > 0$ . We can easily see that a completely developed spiral pattern obtained at  $t \rightarrow \infty$  in figure 4 satisfies (7) using the four spiral curves and the reduction above. Note that we cannot explain the whole evolution of the solution shown in figure 4 because the initial data do not satisfy the equality condition of values on four spirals. We add a note that there is a reversely winding spiral obtained from a mirror image of the above spiral curves.

There are many other evolutionary patterns satisfying (7) with other families of curves and the same reduction. Figure 10 shows such examples. If we assume all values are the same on each curve for initial data, we can obtain a double-target pattern from figure 10(a) and a double-spiral one from (b). We can easily see that some targets and/or spirals can coexist like these examples and it is true for various reaction–diffusion systems. However, if we set two cores of targets with value 1 and with value 2 apart from each other, their interaction is complicated and the target pattern with value 2 often destroys that with 1 after enough time.

#### 4. Other models

In the previous section, we have shown a symmetry of (2) makes stable patterns tracing coordinate curves. However, this symmetry is not peculiar to (2) and there are other max-plus models showing the patterns. For example, a model equation

$$U_{ij}^{t+1} = \max(U_{i-1j}^t, U_{i+1j}^t, U_{ij-1}^t, U_{ij+1}^t, U_{ij}^t) - U_{ij}^{t-1} \quad (11)$$

also gives the travelling wave, target pattern, spiral pattern and their multiple patterns. The difference from (2) is a lack of the term  $-U_{ij}^t$  in the right-hand side. This equation can be reduced to

$$F_n^{t+1} = \max(F_{n-1}^t, F_n^t, F_{n+1}^t) - F_n^{t-1} \quad (12)$$

using the same assumption as in the previous section. Since a travelling wave solution satisfies

$$G_{n-1} + G_{n+1} = \max(G_{n-1}, G_n, G_{n+1}) \quad (13)$$

its local value pattern is  $0ba$  or  $ab0$  where  $a \geq 0$  and  $a \geq b$ , or  $aa + bb$  where  $a \geq 0$  and  $b \geq 0$ . It means that a local pattern  $0c0$  ( $c \geq 0$ ) cannot be allowed and  $0cc0$  is possible. Therefore the width of localized waves becomes wider. Figure 11 shows a periodic double-spiral pattern with period 4. Note that coordinate curves are of the same type of those in figure 10(b) and the width of spiral becomes wider than that in figure 4.

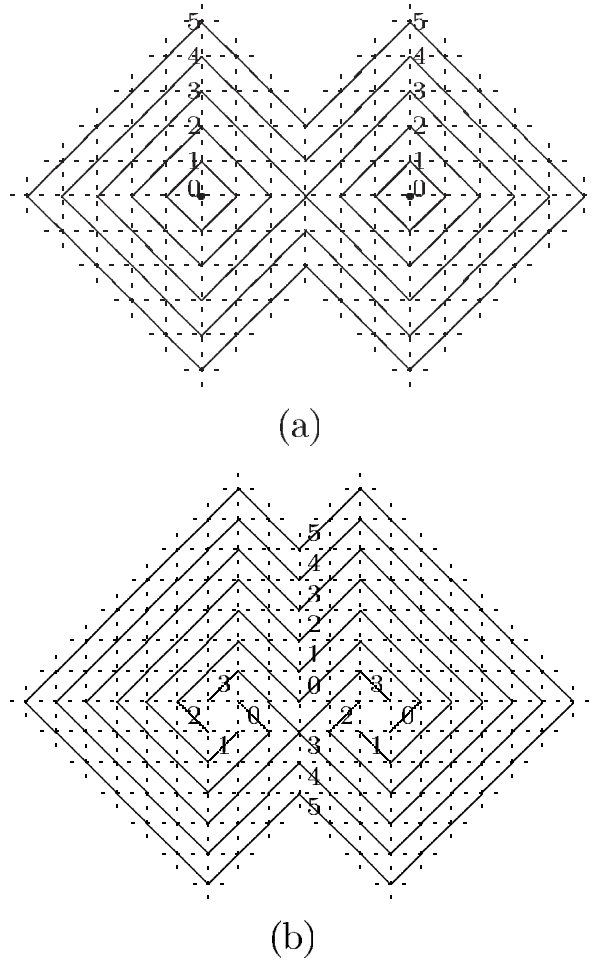


Figure 10. Curves for (a) a double target, (b) a double spiral.

Another example of a model is the following:

$$U_{ij}^{t+1} = \max(U_{i-1j}^t, U_{i+1j}^t, U_{ij-1}^t, U_{ij+1}^t, U_{ij}^t, U_{ij}^{t-1}) - U_{ij}^{t-1}. \tag{14}$$

An additional term  $U_{ij}^{t-1}$  is introduced into the max term of (11). Using coordinate curves, this equation reduces to

$$F_n^{t+1} = \max(F_{n-1}^t, F_n^t, F_{n+1}^t, F_n^{t-1}) - F_n^{t-1}$$

and travelling wave solutions satisfy the same equation as (13). Since the max term of (14) includes  $U_{ij}^{t-1}$ , we derive  $U_{ij}^{t+1} \geq 0$ . Moreover, we easily see that  $U_{ij}$  at time  $t + 1$  cannot exceed the maximum value among those at time  $t$ . Therefore, if  $0 \leq U_{ij}^0 \leq L$  and  $0 \leq U_{ij}^1 \leq L$  where  $L$  is a positive integer,  $U_{ij}^t$  is also. Especially, if  $U_{ij}^0$  and  $U_{ij}^1$  are all 0 or  $L$ ,  $U_{ij}^t$  is also. In this sense, (14) constructs a CA depending on initial data. Since the solution to (11) shown in figure 11 includes only 0 and 1, it also becomes a solution to (14).

Moreover, if all  $U_{ij}^t$  are always 0 or  $L (> 0)$  as described above, we can show the existence of ‘tough’ cores of target and spiral patterns. In this case, if  $U_{ij}^{t-1} = 0$  and  $U_{ij}^t = L$ , then

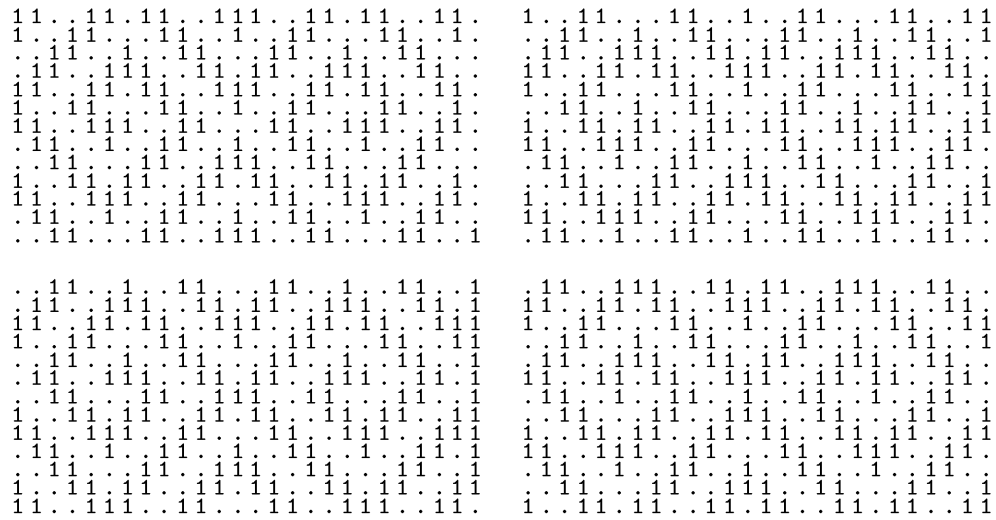


**Figure 11.** Double-spiral pattern given by (11). It is also a solution to (14).

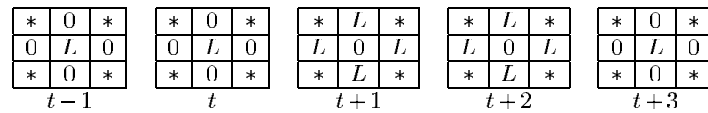


**Figure 12.** Core of the target pattern of (14). \* denotes 0 or  $L$ .

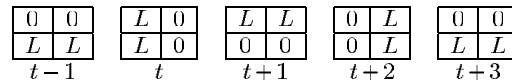


**Figure 13.** Core of the spiral pattern of (14).

$U_{ij}^{t+1} = L$ ,  $U_{ij}^{t+2} = 0$  and  $U_{ij}^{t+3} = 0$  are obtained from (14). Moreover, if  $U_{ij}^{t-1} = U_{ij}^t = 0$  and at least one of  $U_{i\pm 1j}^t$  and  $U_{ij\pm 1}^t$  is  $L$ , then  $U_{ij}^{t+1} = L$  is derived. Therefore, an evolution of a local pattern shown in figure 12 is stable and periodic with period 4. This becomes the core of the target pattern because the value  $L$  appears repeatedly at the centre point and its copies propagate to neighbouring sites. Another tough core is shown in figure 13 and it is also periodic with period 4. This is a core of spiral pattern and we can observe the same cores in figure 11.

### 5. Concluding discussions

In this paper, we presented a max-plus model (2) showing a pattern formation mechanism. It gives travelling waves, target patterns and spiral patterns. Target and spiral patterns are stable as are multiple target or spiral patterns. The remarkable feature of the model is that we can show such patterns by exact solutions using the reduction of the high-dimensional equation to a lower dimension with coordinate curves, as we often do for high-dimensional differential equations.

We also showed two other models (11) and (14) by removing or adding a few terms. Despite the modification, target and spiral patterns survive and their solutions are derived by

a similar reduction process. In the latter model, we showed it can construct a CA under a restriction and the evolution of the core is not affected by surrounding sites. It is interesting that similar types of equations give similar dynamics. This is generally true for the real reaction–diffusion systems and their mathematical models.

Next, we give interesting future problems related to the above models. The first problem is analysing a general dynamics from arbitrary initial data. We showed only specific patterns from selected initial data made from two integer values. Our numerical simulations from more general data suggest a complicated evolutionary dynamics and sometimes a chaotic behaviour. Note that our models give a stable basic pattern of an arbitrary value. If  $U_{ij}^t$  is a solution, then  $c U_{ij}^t$  is also. On the other hand, a value of the uniform solution to known differential models changes between two stable values periodically, and the bottom and top areas of a localized wave take either of the values. We consider that this difference in the property of our models from the differential models reflects the complex dynamics of our models. In this sense, the physical interpretation of our models should be discussed.

Our models can propose a clear analysis on various characteristic patterns. Exact solutions of the whole region including the core area are rarely obtained for differential systems. Our models are fully discrete and it makes analysis easier. Though considering this advantage, reduction of the equation with coordinate curves is a parallel procedure to those performed for differential systems. Note that known CA models showing the patterns are usually described by a Boolean operation or procedural words and such an analysis is rarely successful. We hope a strong link exists between our models and differential systems utilizing the above features of our models, such as integrable max-plus equations.

We make two remarks below in order to suggest this link. First, consider a finite difference equation

$$g_{n-1}g_n g_{n+1} = g_{n-1} + g_n + g_{n+1}. \tag{15}$$

If we use a transformation  $g_n = e^{G_n/\varepsilon}$  and take a limit  $\varepsilon \rightarrow +0$ , we get (7) using formulae (1). Moreover, (15) reduces to  $\theta_{n-1} + \theta_n + \theta_{n+1} = k_n\pi$  where  $g_n = \tan \theta_n$  and  $k_n$  is an arbitrary integer depending on  $n$ . One of the solutions to this equation is  $\theta_n : \dots \frac{\pi}{4}, \frac{\pi}{4} + \delta, \frac{\pi}{2} - \delta, \frac{\pi}{4}, \frac{\pi}{4} + \delta, \frac{\pi}{2} - \delta, \dots$ . If we use  $\delta = e^{-1/\varepsilon}$  and take a limit  $\varepsilon \rightarrow +0$ , we obtain  $G_n : \dots 001001 \dots$ . This is a solution to (7). Though we cannot give a general solution of  $G_n$  from (15), we can consider (15) is a suggestive example to show a relationship between continuous and discrete models.

Secondly, consider the following difference equation:

$$u_{ij}^{t+1} + u_{ij}^t + u_{ij}^{t-1} = \log[\alpha(e^{u_{i+1j}^t} + e^{u_{i-1j}^t} + e^{u_{ij+1}^t} + e^{u_{ij-1}^t}) + \beta e^{u_{ij}^t}] \tag{16}$$

where  $\alpha$  and  $\beta$  are positive constants. If we use a transformation  $u_{ij}^t = U_{ij}^t/\varepsilon$  and take an ultradiscrete limit  $\varepsilon \rightarrow +0$ , we obtain (2) directly. Moreover, if we assume  $u_{ij}^t = v(hi, hj, ht)$  and  $h \sim 0$ , we obtain

$$v_{tt} \sim \frac{\alpha}{4\alpha + \beta} (\Delta v + |\nabla v|^2) + \frac{1}{h^2} (\log(4\alpha + \beta) - 2v). \tag{17}$$

When we use initial data of  $u_{ij}^t$  corresponding to  $U_{ij}^t$  with finite  $\varepsilon$  and calculate a time evolution of (16) numerically, we can observe patterns described in the previous sections if  $\varepsilon$  is small enough. However, the patterns do not survive eternally and they disappear after a long time. When  $\varepsilon$  is not small ( $\varepsilon \sim 1$ ), the patterns disappear more quickly. Moreover, we cannot observe the patterns surviving for a long time in the numerical calculations of (17).

Equation (16) is not a unique equation reducing to (2) and we can make many other examples. Therefore, it is an important future problem to find a difference and differential equations which are directly related to (2) through ultradiscretization and give a similar pattern mechanism.

## References

- [1] Baccelli F, Cohen G, Olsder G J and Quadrat J P 1992 *Synchronization and Linearization* (New York: Wiley)
- [2] Tokihiro T, Takahashi D, Matsukidaira J and Satsuma J 1996 *Phys. Rev. Lett.* **76** 3247
- [3] Hirota R, Iwao M, Ramani R, Takahashi D, Grammaticos B and Ohta Y 1997 *Phys. Lett. A* **236** 39
- [4] Ramani R, Takahashi D, Grammaticos B and Ohta Y 1998 *Physica D* **114** 185
- [5] Tokihiro T, Takahashi D and Matsukidaira J 2000 *J. Phys. A: Math. Gen.* **33** 607
- [6] Nishinari K and Takahashi D 1998 *J. Phys. A: Math. Gen.* **31** 5439
- [7] Wolfram S 1986 *Theory and Applications of Cellular Automata* (Singapore: World Scientific)
- [8] Meron E 1992 *Phys. Rep.* **218** 1
- [9] Winfree A T 1974 *Sci. Am.* **230** 82
- [10] Moe G K, Rheinboldt W C and Abildskov J A 1964 *Am. Heart J.* **67** 200
- [11] Greenberg J M and Hastings S P 1978 *SIAM J. Appl. Math.* **34** 515
- [12] Greenberg J M, Hassard B D and Hastings S P 1978 *Bull. Am. Math. Soc.* **84** 1296
- [13] Greenberg J M, Greene C and Hastings S P 1978 *SIAM J. Algebr. Discrete. Methods* **1** 34
- [14] Hartman H and Tamayo P 1990 *Physica D* **45** 293
- [15] Gerhardt M and Schuster H 1989 *Physica D* **36** 209
- [16] Gerhardt M, Schuster H and Tyson J J 1990 *Physica D* **46** 392
- [17] Gerhardt M, Schuster H and Tyson J J 1990 *Physica D* **46** 416